Comparative anatomical study of retinal ganglion cell topography in predatory birds

（猛禽類における視神経節細胞の分布に関する比較解剖学的研究）

2022年 9 月

岩手大学大学院

獣医学研究科

西村　裕之

CONTENTS

General Introduction

The eyes of vertebrates developed under phylogenetic and evolutionary constraints (Walls,1942; Land and Fernald, 1992) and exhibit specific adaptations to the surrounding environment and way of life, such as in lizards (Wilhelm and Straznicky, 1992), fishes (Fishelson et al., 2004), primates (Kirk, 2004), birds (Hall and Ross, 2007) and aquatic mammals (Mass and Supin, 2007).

In general, the mammalian eye is spherical which is mechanically robust and facilitates rotation of the eye in its orbit. On the other hand, the bird's eye is far from spherical. The concavity around the cornea saves the space and weight of the eye. The mechanical weakness of the bird's eye is stiffened by the scleral ossicles which also provide a firm origin for the striated and rapidly acting muscles of accommodation (Walls, 1942; Pumphrey, 1961), i.e., Brucke's muscle and Crampton's muscle. The shapes of the bird's eye vary and have been morphologically categorized into the following three groups: the 'flat,' 'globose,' and 'tubular' types (Walls, 1942; Pumphrey, 1961; Fig. 1). Tubular- and globose-type eyes are observed in owls and raptors, respectively. Flat-type eyes are the most common in other species (Walls, 1942; Pumphrey, 1961). Birds have excellent visual sensitivity, and the size of their eyes relative to their body size is larger than in other vertebrates (Howland et al., 2004; Kiltie, 2000). Among birds, raptors and owls have more giant eyes concerning their body size than other species, which indicates the significance of the vision of the species (Hughes, 1977; Johnsgard, 1988; Brooke et al., 1999; Garamszegi et al., 2002; Howland et al., 2004; Burton, 2008).

On the one hand, it is proposed that differences in optical design can also be interpreted concerning ecological and behavioral parameters (Martin, 1994; Schmitz, 2009). The relationship between eye morphology and activity pattern has been the subject of comparative studies in vertebrates (Brooke et al., 1999; Kiltie, 2000; Garamszegi et al., 2002; Thomas et al.,

2002, 2004; Kirk, 2004; Thomas et al., 2006; Kirk, 2006a, b; Ross and Kirk, 2007; Hall and Ross, 2007; Ross et al., 2007; Hall, 2008; Heesy and Hall, 2010; Schmitz and Motani, 2010; Motani and Schmitz, 2011). Previous studies focused on the analysis of morphological features that represent an estimate for *f*-number, i.e., a ratio of aperture diameter and posterior nodal distance. The measurements of the eye used in these studies include the corneal diameter (C) and the axial length (A; Fig. 2). Pupil size, that is aperture, controls the amount of light entering the eye, which affects the brightness of the retinal image, and is placed an upper limit on dilation by corneal size (Malmström and Kröger, 2006; Martin, 1983; Martin and Osorio, 2008). Posterior nodal distance (PND) affects the size of the image of an object on the retina and is the constant value of axial length (A) across vertebrates (PND = 0.6 × A; Hughes, 1977; Martin, 1982; Murphy and Howland, 1987). Thus, corneal diameter and axial length are proxies for maximum pupil diameter and PND, respectively. The relative corneal diameter to the axial length, that is the C:A has been used as an index for the diel activity of the species in primates (Kirk, 2004, 2006a, b; Ross and Kirk, 2007). That is, the C:A is higher in the nocturnal species, lower in the diurnal species ,and intermediate value in the cathemeral and crepuscular species. Hall and Ross (2007) demonstrated that those relationships can be adapted to 459 non-passerine bird species, however, the C:A on the boundaries of the respective ranges of categories seem to be obscure. Moreover, few studies present the morphological adaptive features of globose- and tubular-type eyes to ecological habits.

The priorities and interests of the visual system in vertebrates are apparent at the level of ganglion cells (Stone, 1983; Land and Fernald, 1992). Retinal ganglion cells (RGCs) receive signals from photoreceptors and those data are compressed before being transmitted to the visual center of the brain (Shapley and Perry, 1986; Kolb et al., 2001). The high-density area of RGCs is known as a retinal specialization (Meyer, 1977), which provides higher spatial resolving power in the discrete visual field (Collin, 1999; Hughes, 1977). Diverse types of

retinal specializations have been identified across vertebrates, i.e., foveae, *areas of retina temporalis*, and visual streaks, which vary in number, size, shape, and position in the retina (Collin, 1999, 2008; Hughes, 1977).

A visual streak is an elongated area of high RGC density stretching across the retina, which is thought to allow a species to view a panoramic field, without the need for extensive eye or head movement (Collin, 1999, 2008; Hughes, 1977). Hughes (1977) hypothesized that the visual streak is common to terrestrial species whose field of view is not completely obscured by nearby vegetation, and the terrain surface is overt above the stream bed to a fish, or above the sea to a flying or floating bird; that is, the 'terrain' theory. Visual streak is observed across a wide range of taxa, e.g., ungulates (ox and sheep; Hebel, 1976), turtle (Peterson and Ulinski, 1979), kangaroo (Dunlop et al., 1987), reef teleost (Collin and Pettigrew, 1988), lizard (Wilhelm and Straznicky, 1992), hyena (Calderone et al., 2003), and birds including several species of birds inhabiting in visually open habitats; peafowl (Hart, 2002), crow (Rahman et al., 2006), ostrich (Rahman et al., 2010), Canada geese (Fernández-Juricic et al., 2010), waterfowl (Lisney et al., 2013b) and hummingbird (Lisney et al., 2015). Visual streak occasionally contains foveae, a region where the inner retinal layer is depressed (Walls, 1942). Foveae are divisible into two fairly distinct classes based on the form of the depression (Pumphrey, 1948). The shallow class includes the fovea of anthropoids, and also the temporal fovea of some birds. On the one hand, the fovea of fish, reptiles and central fovea of birds belong to the deep class. The functional role of fovea has been proposed, such as optical magnifying effect, improvement of spatial resolution, improvement of detection and fixation on small moving objects (Mitkus et al., 2018). Most predatory raptors have two foveae (central and temporal fovea), while carrion-eating raptors have only the deep central fovea (Inzunza et al., 1991; Lisney et al., 2013a). Although the functional role of fovea remains unclear, it has been speculated that foveae play a significant role in predatory behavior.

On the other hand, the classification of RGCs has been explored in cat (Bishop and O'Leary, 1938, 1940, 1942; Kuffler, 1953; Cleland et al., 1971; Boycott and Wässle, 1974; Rowe and Stone, 1976). According to the studies on the properties of cellular response to photic stimuli, RGCs of the cat are functionally classified into three groups, termed Y-, X- and W-cells (Boycott and Wässle, 1974; Enroth-Cugell and Robson, 1966; Stone and Hoffman, 1972; Stone and Fukuda, 1974). The morphological classification of cat's RGCs was proposed by Boycott and Wässle (1974), who distinguished three principal cell groups, termed α-, β-, and γ-cells. These cell groups were distinct in the soma size, dendritic morphology, and axonal caliber. It is suggested that α-cells correspond to Y-cells, β-cells to X-cells, and γ-cells to W-cells (Boycott and Wässle, 1974). Finally, it is suggested that Y(α)-cells subserve movement vision, that X(β)-cells subserve high-resolution pattern vision, and that W(γ)-cells subserve ambient vision (Stone, 1983). In birds, the morphological classification of RGCs was performed by Nissl's staining method (Ueshima and Uehara, 1983), a neuronal tracer method in a chick retina (Chen and Naito, 1999), and the Horse Radish Peroxidase retrograde labeling method in the Japanese quail (Ikushima et al., 1986). The findings obtained in those studies indicated similarities in the classification of RGCs in cats. Morphological classes of RGCs subserve different functional roles and are closely related to the topographical specialization of the retina (Stone, 1983). Therefore, it is assumed that the topography of the RGC classes would relate to the functional role of the retinal area.

Raptors and owls are renowned for their high visual performance, and the RGC topography maps exist for six species of raptors; American kestrel (*Falco sparverius*), black-chested buzzard-eagle (*Geranoaetus melanoleucus*), chimango caracara *(Phalcoboenus chimango*), Andean condor (*Vultur gryphus*), black vulture (*Coragyps atratus*), and turkey vulture (*Cathartes aura;* Inzunza et al., 1991; Lisney et al., 2013a); and for nine species of owls: northern saw-whet owl *(Aegolius acadicus*), short-eared owl (*Asio flammeus*), burrowing owl

(*Athene cunicularia*), snowy owl (*Bubo scandiacus*), great-horned owl (*Bubo virginianus*), great grey owl (*Strix nebulosa*), barred owl (*Strix varia*), northern hawk owl (*Surnia ulula*) and barn owl (*Tyto alba*) (Linsey et al., 2012). Owls and raptors have tubular- and globose-type eyes, respectively, while their ecological habits, i.e., the habitat preference, the foraging behavior, and the diel activity, differ from each other among those species. In spite of the previous studies which presented the eye morphology and the RGCs' topography maps of raptors and owls, it remains unclear how the eyes of raptors and owls are affected by ecological habits.

In the present study, I prepared the RGC maps of owls and raptors to obtain the differences in the retinal topography which are supposed to be adaptable to varied ecological habits. To obtain a more detailed understanding of the morphological diversity of the tubular- and globose-type eye, I performed macroscopic measurements of the eyes of two owls and one raptor species. In addition to macroscopic observation, I also conducted a histological analysis of RGCs using whole-mount preparations by Nissl's staining method to obtain the retinal specialization. Furthermore, I tentatively classified the RGCs based on soma size and appearance. Finally, the topography maps of the RGC classes were prepared to discuss the functional roles of the retinal parts where those cells were distributed.

In Chapter 1, the eyes of the short-eared owl (*Asio flammeus*) and the Japanese scops owl (*Otus semitorques*) were investigated as the typical tubular-type eye. As both species belong to Strigidae, they are qualified for comparison of the eye morphology and retinal topography of the species with different ecological habits from each other. Additionally, the morphological adaptation of the eye was also discussed. The RGCs were tentatively classified based on size and appearance, and the map of those cells was prepared to discuss the functional property of those cells.

In Chapter 2, the retinal topography in the northern goshawk (*Accipiter gentilis*), which has

a globose-type eye, was investigated in the same way in Chapter 1. As a representative of diurnal birds of prey, the retinal specialization of the northern goshawk showed the adaptation to the predatory behavior which was remarkably different from those of owls.

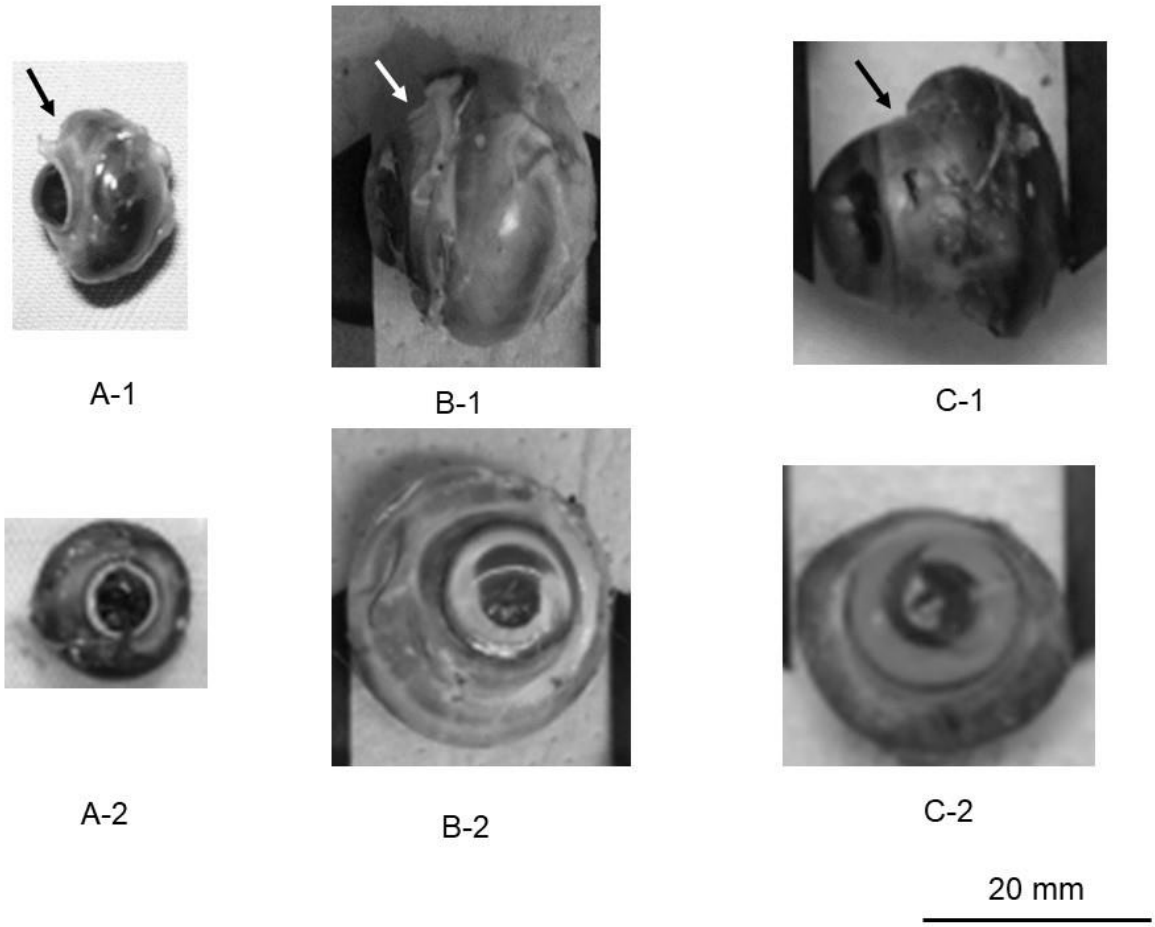

Fig. 1. Characteristic shapes of bird's eye

Upper row: nasal view; Lower row: frontal view of the eyes.

A: flat type, Oriental turtle dove (*Streptopelia orientalis*)

B: globose type, Northern goshawk (*Accipiter gentilis*)

C: tubular type, Short-eared owl (*Asio flammeus*)

The eyes of birds are morphologically classified into three types. The globose and the tubular type of eyes are specific for raptors and owls, respectively. The flat type of eye is most common for the other species. Scleral ossicles (arrows) characterize the specific shape of eye in each species. The globose type of eye enlarges the posterior segment which includes the retina. The tubular type of eye elongates in the anteroposterior direction.

Bar represents 20 mm.

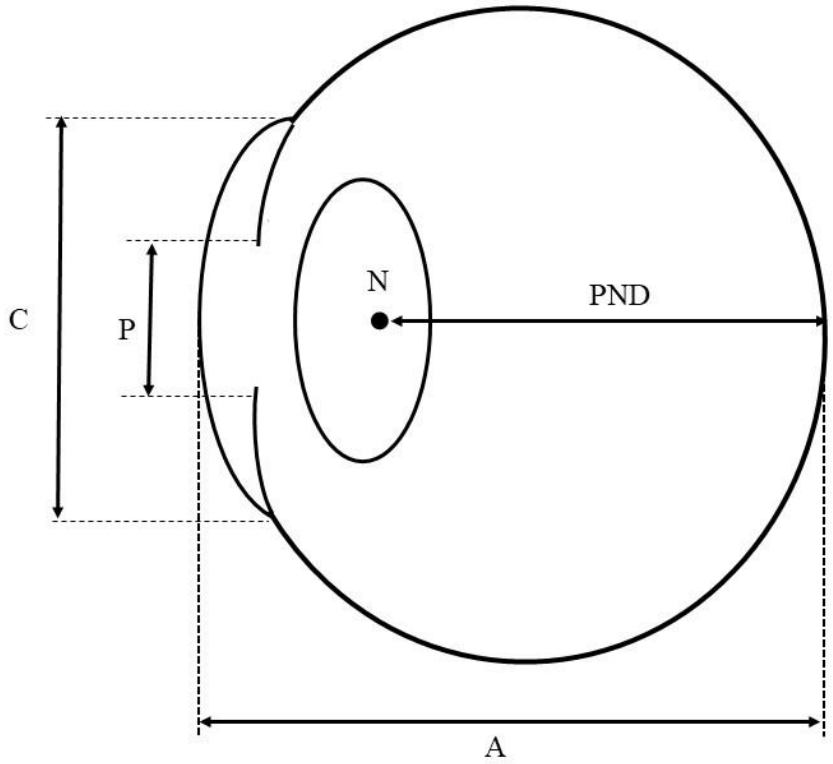

Fig. 2. A schematic eye of the vertebrates

Corneal diameter (C) places an upper limit on the pupil dilation which allows the amount of light entering into the eye. Posterior nodal distance (PND) is the constant value of the axial length (A), which is $0.6 \times$ A, across the vertebrates (Hughes, 1977; Martin, 1982; Murphy & Rowland, 1987). Longer PND enlarges the image projected onto the retina. It is noticeable that the dimensions of the eye reveal the functional property of the eye.

C, Corneal diameter; P, Pupil size; N, Nodal point; A, Axial length; PND, Posterior nodal distance

Chapter 1

Adaptive features of the eye to the ecological habit of the short-eared owl (*Asio flammeus*) and Japanese scops owl (*Otus semitorques*)

Introduction

According to the general description in the literature, owls develop on every continent except Antarctica and appear to have evolved to the well-defined ecological niche of each species with different activity patterns and habitat preferences. Forests and woodlands are highly utilized by owls of all major sizes (Johnsgard, 1988). Owls are divided into two families, i.e., seventeen species of barn owls (*Tytonidae*) and 227 species of typical owls (*Strigidae*) (Bird Life International, 2019). Insectivorous species of owls are those that occur in fairly open, arid environments, whereas larger owls concentrating primarily on birds and mammals are associated with boreal to arctic habitats (Johnsgard, 1988).

Vision is a particularly important sensory modality for owls in general (Walls, 1942; Pumphrey, 1961; Martin, 1986; Murphy and Howland, 1987). The eyes of owls are so large that they are in contact with the mid-line of the skull (Fig. 3). As their eyes are fixed into the sockets by connective tissue, owls are unable to move their eyes. Thus, owls must move their heads to bring objects into focus at the points of high-resolution retinal area (Johnsgard, 1988). Besides its enormous relative size, an owl's eye has remarkable characteristics, which are a tubular shape and shows high visual performance (Walls, 1942; Martin, 1986). Therefore, it is probable that the eyes of owls are strongly affected by the ecological habit of the species.

Among the owl species living in Japan, a short-eared owl (*Asio flammeus*) is a migratory bird distributed across Asia, Europe, and North and South America, inhabiting grassland and wetland and is active at dusk and dawn (Johnsgard, 1988). On the other hand, a Japanese scops owl (*Otus semitorques*) is distributed across East Asia and is an altitudinal migrant that inhabits

forests and is active at night (IUCN, 2021).

In Chapter 1, I conducted a macroscopic analysis of the eye, and histological analysis of RGCs using whole-mount preparations to obtain the adaptive features of the tubular-type eye to the ecological habit of the species.

Materials and Methods

Materials

One short-eared owl (male, body weight of 280.0 g, body length of 33 cm) and one Japanese scops owl (male, body weight of 100.0 g, body length of 23 cm) were used in the present study. Both owls had been housed in the Akita Prefectural Bird and Beast Conservation Center for years and were incapable of living in the wild. All experimental procedures were practiced in accordance with the Guide for the Care and Use of Experimental Animals of Iwate University (A201847, A202127). Sodium pentobarbital (64.8 mg/ml) was used for euthanasia by intraperitoneal injection (Carpenter et al., 2001). The short-eared owl was immediately immobilized by 0.5 ml of the drug; however, cardiac arrest was not confirmed for 10 minutes. The heart immediately stopped beating after another injection of 0.3 ml of the drug. In the Japanese scops owl, cardiac arrest was confirmed immediately after the injection of 0.5 ml of the drug.

Macroscopic observations

After respiration and heartbeat had both ceased, each eye was dissected, and the connective tissue was removed and weighed. Before removing the eye, I painted a small dot on the temporal part of the scleral ossicle to orient the eye in the right position. To calculate the eye shape, I measured the corneal diameter (C) and axial length (A) of the eye. I measured the corneal diameter along two perpendicular planes, i.e., the superior-inferior and nasal-temporal planes, using digital calipers. The corneal diameter was measured at the corneoscleral junction. The axial length was assessed by the distance between the vertex of the cornea and the posterior part of the eye. These values were used to calculate the eye shape, which was defined as the ratio of C:A (Hall and Ross, 2007).

Retinal whole-mount preparations

The eye was dissected at the ora serrata, and the retina was removed and stored in fixative fluid (4% paraformaldehyde in 0.1 M phosphate-buffered saline solution, pH 7.4) at 4°C. After fixation, the retina was mounted onto a gelatinized slide and air-dried at room temperature for 24 hours. It was then defatted by 100% ethanol, rehydrated through a descending series of ethanol (90, 70, and 20%), and stained with 0.1% cresyl violet at 37°C for 1 hour, followed by dehydration through an ascending series of ethanol (20, 70, 90, and 100% twice). The slide was cleared in xylene and cover-slipped using a synthetic mounting medium (MGK-S, Matsunami, Tokyo). A transparent grid of 1×1 mm was attached to the slide glass on the opposite side of the retina. We scanned the slide and outlined the retina using Microsoft PowerPoint (Microsoft, Redmond, WA, USA). RGCs possessing an irregularly shaped soma with Nissl substance and a distinct nucleus (Ehrlich, 1981) were observed under a compound microscope with a ×100 objective lens. An eyepiece graticule (10×10) was attached to the microscope to observe RGCs. As the RGCs were found to be varied in size and shape, they were tentatively classified into the small-, medium-, and large-sized cells based on soma size. I selected every alternate square (100×100 μm) in the grid (1×1 mm) and counted the number of each size of RGCs within the boundaries of the 10×10 graticule. Sample locations were 336 and 428 in the short-eared owl and Japanese scops owl, respectively. To prevent double-counting I only counted cells within each square grid that touched two sides (Gundersen, 1977; Ullman et al., 2012). Cell counts were converted into the number of cells in square millimeters (cells/mm^2) and plotted in every grid of whole retinas. These grids were painted with gradated gray in twelve steps depending on cell density. RGC isodensity contour plots were drawn using a median filter with the computer software, Photoshop PS5 (Adobe, San Jose, CA, USA).

Results

Macroscopic observations

The eyes of both species were fixed into the sockets and the anterior segments protruded from the frontal face (Fig. 3). The cornea and posterior segments of the eye were connected by elongated scleral ossicles, which characterize the tubular-type eye shape (Fig. 4). Body weight (B) and eye dimensions are shown in Table 1. Eye dimensions, i.e., eye weight (E), corneal diameter, and axial length, were larger in the Japanese scops owl. The ratios of eye dimensions, namely, E:B and A:B, was also larger in the Japanese scops owl; however, C:A was the same in both species, otherwise larger in the short-eared owl (0.694-0.705) than in the Japanese scops owl (0.635-0.701).

Number and distribution of RGCs

The distribution of RGCs was observed in whole-mount preparations (Fig. 5). The estimated total numbers of RGCs were $2{,}342.0\times10^3$ and $4{,}703.0\times10^3$ in the short-eared owl and Japanese scops owl, respectively. RGC densities ranged between 2.4 and 17.4×10^3 (average: 7.0×10^3) cells/mm^2 in the short-eared owl and between 4.7 and 23.1×10^3 (average: 11.0×10^3) cells/mm^2 in the Japanese scops owl. Oval-shaped pecten was observed in the center of the ventral retina in both species. The distribution densities of RGCs in each retinal area of both species were presented in Fig. 6. In both species, the densities in the central area were 14.0×10^3 cells/mm^2 (Fig. 6A, F). In the nasal area, the densities were 5.9×10^3 and 8.8×10^3 cells/mm^2 in the short-eared owl and Japanese scops owl, respectively (Fig. 6B, G). Similarly, those were 12.7×10^3 and 22.7×10^3 cells/mm^2 in the temporal area (Fig. 6C, H), 4.1×10^3 and 7.9×10^3 cells/mm^2 in the dorsal area (Fig. 6D, I), and 7.2×10^3 and 13.4×10^3 cells/mm^2 in the ventral area (Fig. 6E, J) of the short-eared owl and Japanese scops owl, respectively. Isodensity contour plots of RGCs are shown in Fig. 5. Both species possessed an area of high cell density in the

temporal retina. In the short-eared owl, I observed an area that horizontally extended over the retina. In the Japanese scops owl, this area was observed as an oval shape in the dorsal part of the retina, which elongated in the vertical direction.

Soma size and morphology of RGCs

I tentatively classified the RGCs into three groups based on their soma size and appearance in both species (Fig. 7). Small-sized cells (≤5 μm in diameter) were round in shape with darkly stained nuclei. Medium-sized cells (5-10 μm) were round or oval with eccentric nuclei. Large-sized cells (≥10 μm) were polygonal in shape with cytoplasmic Nissl substance and large nuclei. The numbers of each cell group are presented in Fig. 8. In both species, medium-sized cells dominated the first population of RGCs, and their ratios to all RGCs were 56.8% in the short-eared owl and 72.9% in the Japanese scops owl. Similarly, the ratios of small-sized cells to all RGCs were 24.8% in the short-eared owl and 19.4% in the Japanese scops owl, while those of large-sized cells were 18.4% and 7.7% in the short-eared owl and Japanese scops owl, respectively.

The distribution of each cell group is presented in Fig. 9. In both species, the high-density area of each cell group was observed in the temporal retina, except for large-sized cells in the Japanese scops owl. In the short-eared owl, small-sized cells localized in the ventral area with a peak density of 6.8×10^3 cells/mm^2, and large-sized cells localized in the dorsal area with a peak density of 5.8×10^3 cells/mm^2. In the Japanese scops owl, small-sized cells localized in the dorsal area with a peak density of 6.4×10^3 cells/mm^2, while large-sized cells were uniformly distributed in the whole retina at a low density ($0.1\text{-}2.6\times10^3$ cells/mm^2). The distribution of medium-sized cells in both species was consistent with the high neural density area in the whole retina with peak densities of 17.4×10^3 and 20.2×10^3 cells/mm^2 in the short-eared owl and Japanese scops owl, respectively.

Discussion

Functional features of the eye morphology

In the present study, morphological variations in the tubular-type eye were detected in the short-eared owl and Japanese scops owl. Previous studies reported that raptors and owls have larger eyes than average birds of the same weight (Walls, 1942; Pumphrey, 1961; Brooke et al., 1999; Garamszegi, et al., 2002; Hall and Ross, 2007). Therefore, 'globose' and 'tubular' type eyes are larger than the 'flat' type eyes in other species. Since the feeding habits of raptors and owls involve detecting and capturing prey, these species are highly visual-dependent (Poiter et al., 2020). E:B and A:B were larger in the Japanese scops owl than in the short-eared owl; therefore, vision is a more important and sensitive modality for the Japanese scops owl.

It is suggested that the trade-off between corneal diameter and axial length may provide an optimal vision for species in different ecological habits (Poiter et al., 2020). Therefore, it could be assumed that the C:A may provide the aspect of the adaptation of the eye to the ecological habit of the species, such as the demonstration by Hall and Ross (2007). However, the higher C:A in the short-eared owl than in the Japanese scops owl is contrary to the diel activity of the species. While both larger corneal diameter and axial length in the Japanese scops owl suggest that the species exceeds the short-eared owl in visual sensitivity and acuity, which is consistent with the activity time of the two species. Although the C:A might predict the diel activity of the species, both larger corneal diameter and axial length in the Japanese scops owl would show that the species is adaptable to both photopic and scotopic vision, whereas the short-eared owl with a smaller corneal diameter is probably adaptable for photopic vision rather than scotopic vision.

Number and distribution of RGCs

Larger retinal images will be sampled by a greater number of independent sampling units

(i.e., ganglion cell receptive fields; Veilleux and Kirk, 2014). In the present study, the estimated retinal area was 336 and 428 mm^2 in the short-eared owl and the Japanese scops owl, respectively; and the total number and average density of RGCs were larger in the Japanese scops owl. Furthermore, a larger axial length in the Japanese scops owl may produce larger retinal images of the object. Therefore, an image projected onto the retina of the Japanese scops owl appears to be exposed to more RGCs than that of the short-eared owl. The number and distribution density of RGCs in both species suggested that the resolving power of the eyes of the Japanese scops owl is superior to that of the eyes of the short-eared owl. I also found that pecten was situated in an oblique direction with its superior part pointing to the high-density area of RGCs in both species. However, I did not observe any specific relationship between the position of the pecten and the retinal specialization of these species. Both species possess an area of high-density RGCs in the temporal retina, which is consistent with the findings obtained on nine owl species (Lisney et al., 2012). Images in the binocularly visual field projected onto the temporal retina may be sampled by a larger number of RGCs. Therefore, the higher density area of RGCs may enhance the visual acuity of binocular vision in both species.

Although I could not find fovea in both species, it does not necessarily mean that the two owl species lack fovea. In the study of nine owl species, fovea was identified in seven species. However, fovea was not identified in one of two specimens of northern saw-whet owl and one of three specimens of great horned owl (Lisney et al., 2012). The presence of fovea might depend on species and/or individuals in owls.

The organization of the high-density area of RGCs differed between the two owl species. The area observed in the short-eared owl was similar to the visual streak observed in species living in open grasslands, e.g., the barn owl (Wathey and Pettigrew, 1989), Falconiformes species (Inzunza et al., 1991), and the ostrich (Rahman et al., 2010). Short-eared owls are often observed in low flight over marshes or grassy moorlands and occasionally perch on low vantage

points to search for prey (i.e., small rodents, small birds, and insects) in a lower place

(Johnsgard, 1988). Therefore, the horizontal visual streak in the short-eared owl may be an adaptation for living and foraging in open spaces. While the high-density area of RGCs in the Japanese scops owl was observed as an oval shape and was vertically distributed. Japanese scops owls inhabit dense forests and nest in the cavities of tall trees, and perch on lofty trees to search for prey. Thus, the visual field of Japanese scops owls is completely obscured by trees, which is a vertically complex construction. In terms of visual field sampling, a vertical visual streak is functionally interesting in three-dimensional environments (Coimbra et al., 2012). Moreover, the vertical visual streak in the Japanese scops owl would widely view the lower fields in binocular vision. Therefore, the organization of the high neural density area in the Japanese scops owl may be an adaptation for visual fields in enclosed habitats.

Classification of RGCs

Classification of RGCs has been proposed for several species, including mammals and non-mammals (e.g., monkey, rat, rabbit, tree shrew, goat, ground squirrel, frog, toad, eel, and mudpuppy (Stone, 1983)). In birds, the morphological classification of RGCs has been demonstrated in the chick (Ueshima and Uehara, 1983; Chen and Naito, 1999), and in the Japanese quail (Ikushima et al., 1986). The findings obtained in those studies indicated similarities in the classification of RGCs in cats, that is the Y(α)-, X(β)-, and W(γ)-cells. On the other hand, the functional properties of RGCs in birds were reported in the pigeon (Holden, 1977), the tyrant flycatchers (Coimbra et al., 2009), and penguins (Coimbra et al., 2012). In owls, the morphological classification of RGCs was partly performed by the neuronal tracer method in the barn owl, *Tyto alba,* and the burrowing owl, *Speotyto cunicularia* (Bravo and Pettigrew, 1981). However, the topography of classified RGCs in the owls remain unclear.

Since differences were observed in the morphology, localization, and population of the

tentative three cell groups in the present study, I considered those cell groups to be different cell classes. Therefore, I assumed that each cell group has different functional roles each other, which relate to the ecological habit of the species.

The high-density area of RGCs in the whole retina mostly comprised medium-sized cells in both species. The high neural density area is considered to be an area with high-resolution power (Collin, 1999). Therefore, medium-sized cells appear to play a role in high-resolution pattern vision in both species.

Short-eared owls favor nesting on the ground surrounded by tall grassy vegetation, which effectively camouflages their presence (Johnsgard, 1988). On one hand, Japanese scops owls favor nesting in the cavities of lofty trees and look down on lower fields. When these two species are roosting, the upper and lower visual fields are ambient vision. These visual fields are projected onto the ventral and dorsal retinal areas at which small-sized cells are widely distributed in each species. Therefore, small-sized cells appear to contribute to the ambient vision of both species in the roosting position.

Short-eared owls search for prey in lower visual fields, which are viewed by the dorsal retinal area where the accumulation of large-sized cells was observed. Japanese scops owls hunt in vertically complex constructions of dense forests in the dark, and, thus, prey in the visual field is sampled by the whole retinal area where the large-sized cells are uniformly distributed. Therefore, large-sized cells appear to be involved in the discrimination of prey in the whole visual field.

The results of Chapter 1 suggest that the Japanese scops owl exceeds the short-eared owl in visual sensitivity and acuity, which shows the adaptability to both photopic and scotopic vision. On the other hand, the short-eared owl is more adaptable to photopic vision. The high neural density area showed the adaptation to the inhabitation and foraging behavior of both species.

Table 1. Measurements of body weight and eye shape of the short-eared owl and the Japanese scops owl.

Species	Eye	E (g)	C (mm)	A (mm)	E:B	A:B	C:A
Short-eared owl	Right	2.94	12.85	18.24	0.0105	0.065	0.705
(Body weight, 280.0 g)	Left	2.94	12.70	18.30	0.0105	0.065	0.694
Japanese scops owl	Right	4.55	14.25	20.34	0.0455	0.203	0.701
(Body weight, 100.0 g)	Left	4.52	14.10	21.60	0.0452	0.216	0.635

B, body weight; E, eye weight; C, corneal diameter; A, axial length; E:B, the ratio of eye weight to body weight; A:B, the ratio of axial length to body weight; C:A, the ratio of corneal diameter to axial length.

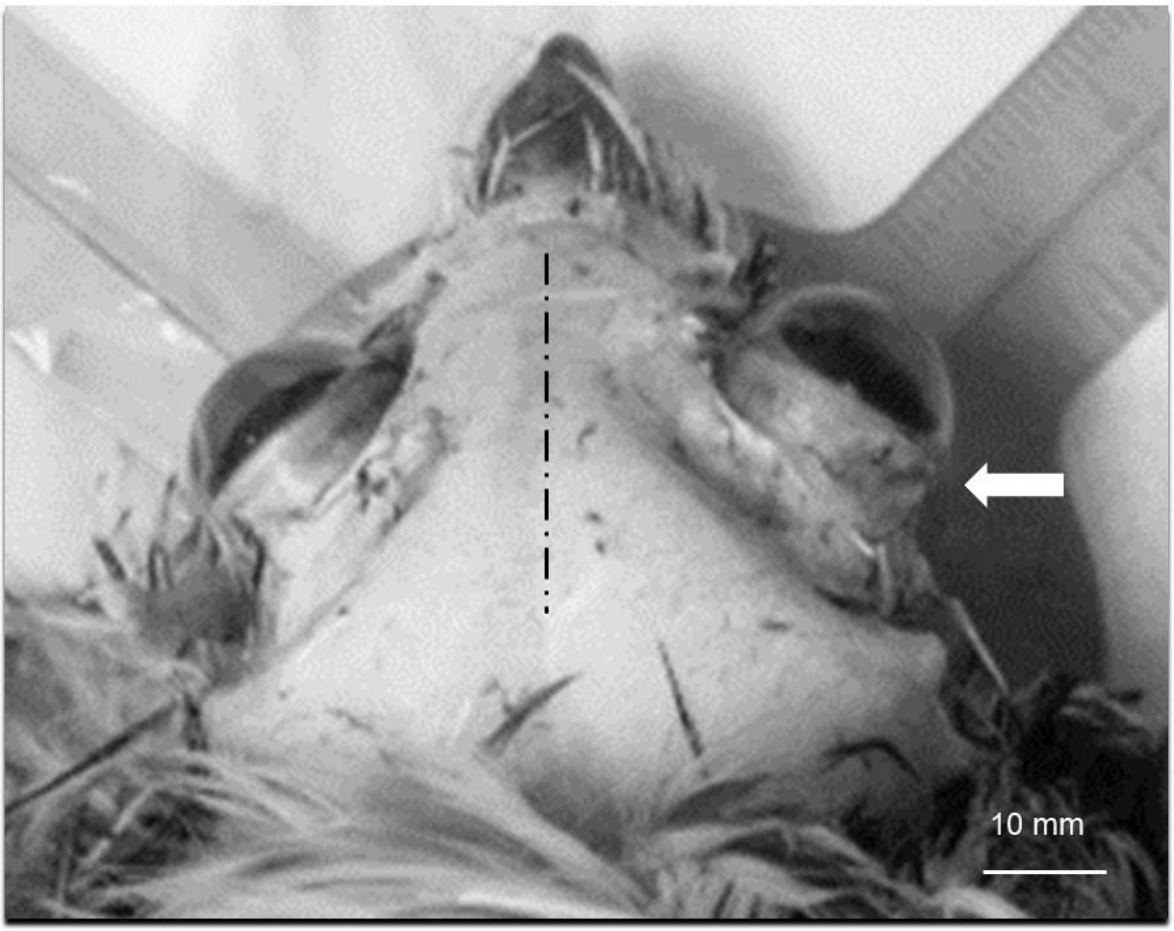

Fig. 3. Dorsal view of the head of the short-eared owl (*Asio flammeus*).

Both eyes are frontally-oriented and protrude from the orbit. The posterior segments are almost in contact at the midline of the head (chain line). Those arrangements of the eye restrain the size of the retina in the posterior segment. Long and robust scleral ossicles (arrow) support the cornea, which provides the species with the characteristic shape of eye and visual function. The plumage of the head, the palpebra, and the skin were plucked and removed for observation.

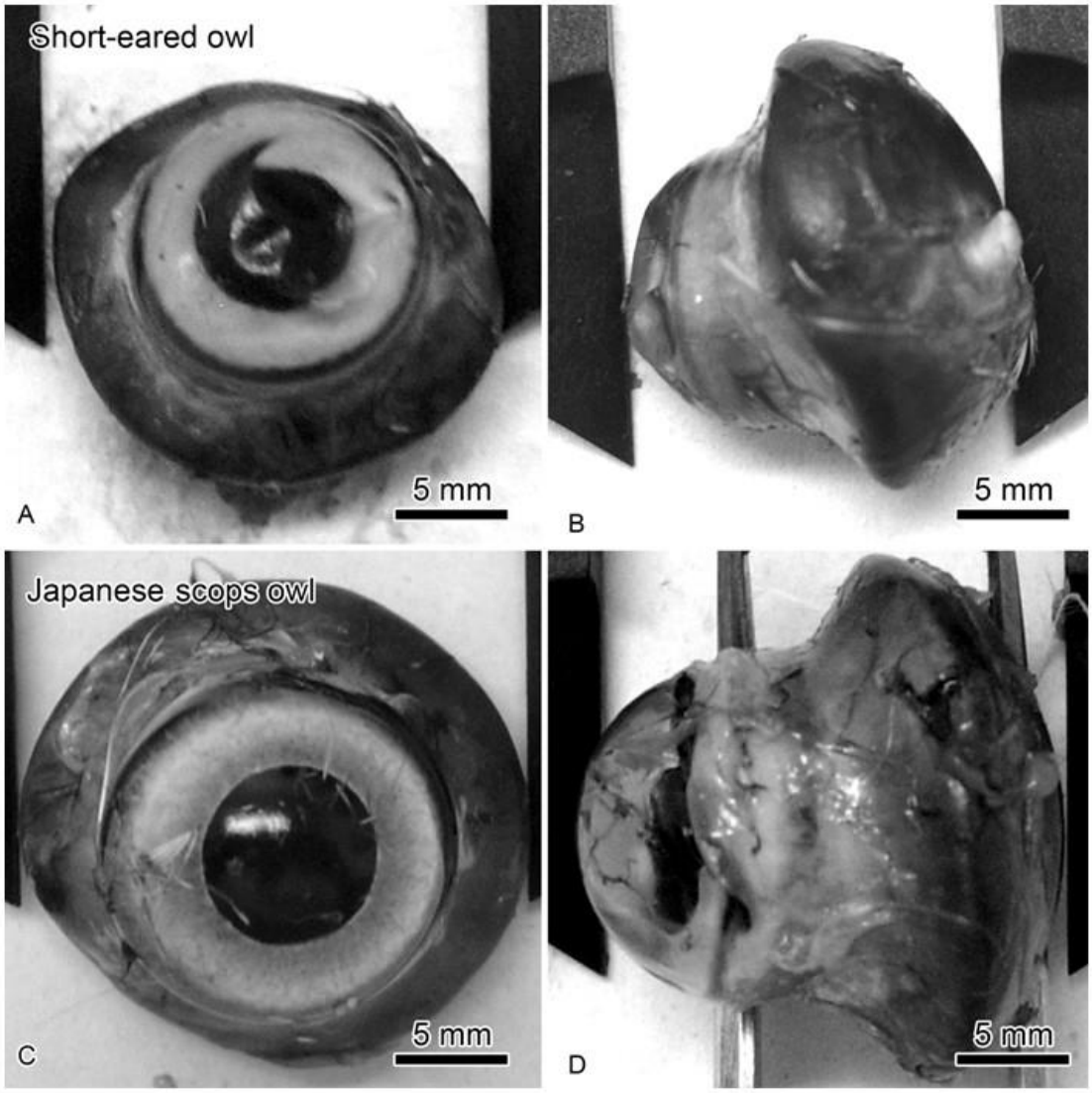

Fig. 4. Frontal (A,C), temporal (B), and nasal (D) views of the eyes of the two species of owl.

A, B Short-eared owl. C, D Japanese scops owl. Bars represent 5 mm. Left eye.

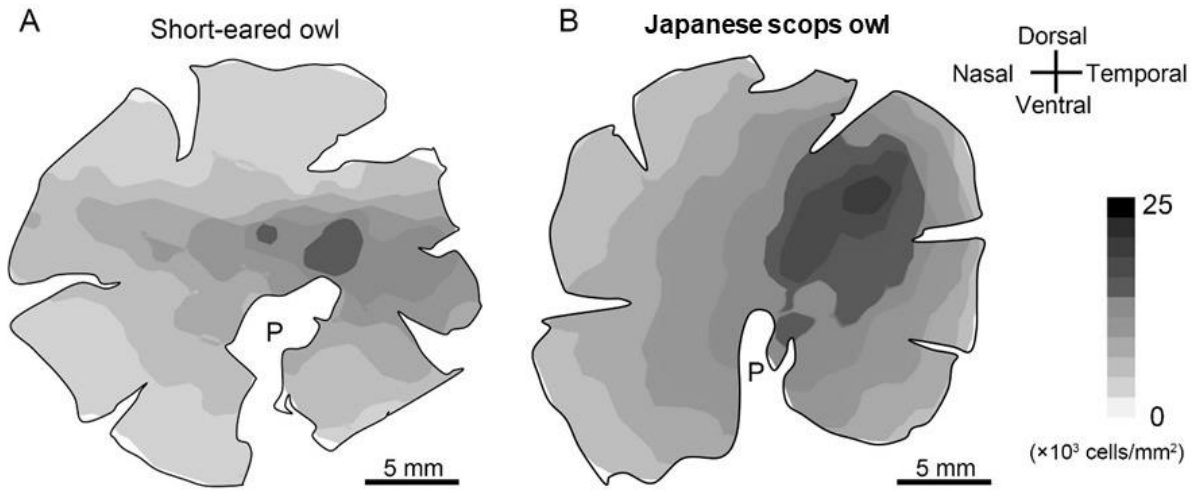

Fig. 5. Isodensity contour maps of RGCs for the short-eared owl (A) and the Japanese scops owl (B).

P, Pecten. The shaded color reveals the density scales of RGCs. Bars represent 5 mm. Left eye. RGC densities range between 2.4 and 17.4×10^3 (average: 7.0×10^3) cells/mm^2 in the short-eared owl and between 4.7 and 23.1×10^3 (average: 11.0×10^3) cells/mm^2 in the Japanese scops owl. The peak density region of RGCs is located in the temporal retina in both species. The horizontal visual streak is observed in the short-eared owl. On the other hand, the high-density area of RGCs extends vertically in the Japanese scops owl.

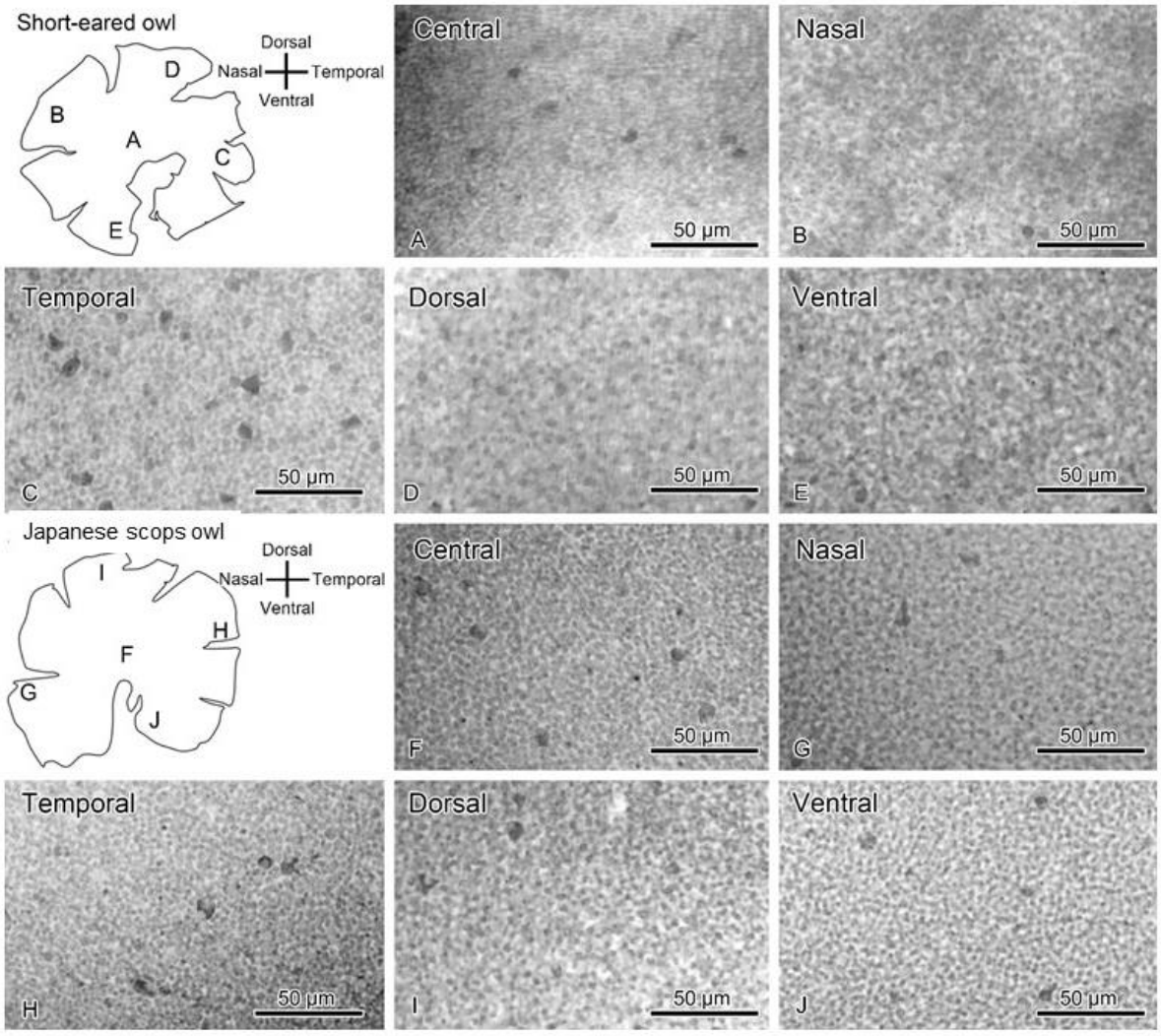

Fig. 6. Nissl-stained RGCs in the short-eared owl (A-E) and the Japanese scops owl (F-J). Low magnification (×20 objective) digital photomicrographs illustrate the RGCs in the central (A, F), nasal (B, G), temporal (C, H), dorsal (D, I), and ventral (E, J) area of the peripheral retina in both species. The large ganglion cells are also observed in the high-density area (A, F). The distance between the central (A,F) and the peripheral area (B,C,D,E,G,H,I,J) is 9-11 mm. Bars represent 50 μm. Left eye.

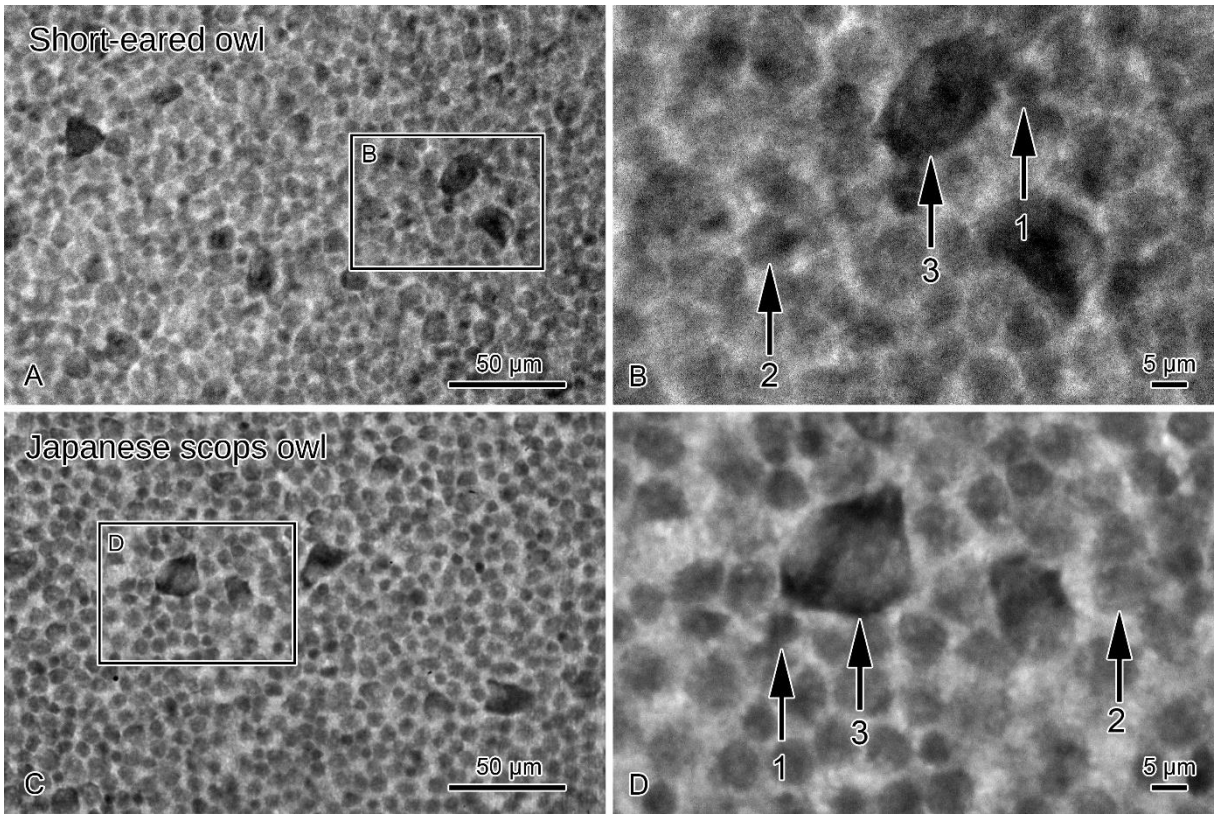

Fig. 7. Differentiation of RGCs in the short-eared owl (A,B) and the Japanese scops owl (C,D).

1, Small-sized cells (≤5 μm in diameter) were round in shape with darkly stained nuclei.; 2, Medium-sized cells (5-10 μm) were round or oval with eccentric nuclei.; 3, Large-sized cells (≥10 μm) were polygonal in shape with cytoplasmic Nissl substance and large nuclei.

The photograph of the enclosed area in (A) and (C) are enlarged and presented as (B) and (D). Bars represent 50 μm in (A) and (C), and 5 μm in (B) and (D). Left eye.

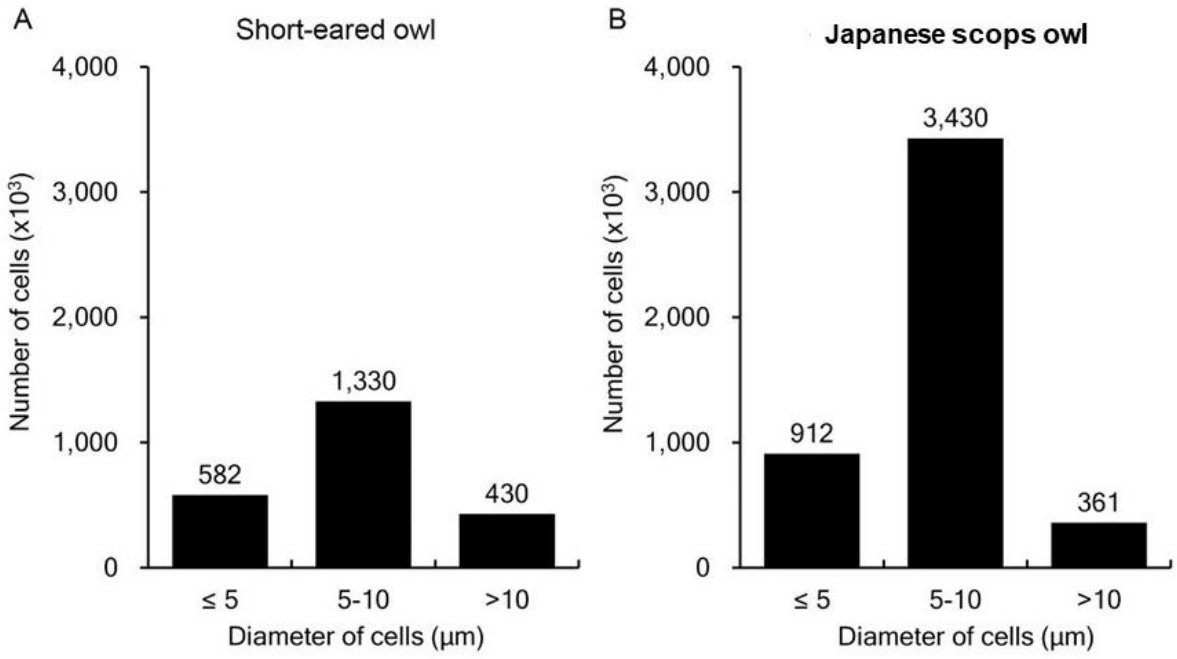

Fig. 8. The histogram of number of each cell group in the short-eared owl (A) and the Japanese scops owl (B).

The cell counts of both species give medium-size cells (5-10 μm in diameter) for a peak range and the large-sized cells for the least.

The population ratio of the small-, the medium-, and the large-sized cells to the total number of RGCs is 24.8%, 56.8%, and 18.4% in the short-eared owl; and 19.4%, 72.9%, and 7.7% in the Japanese scops owl.

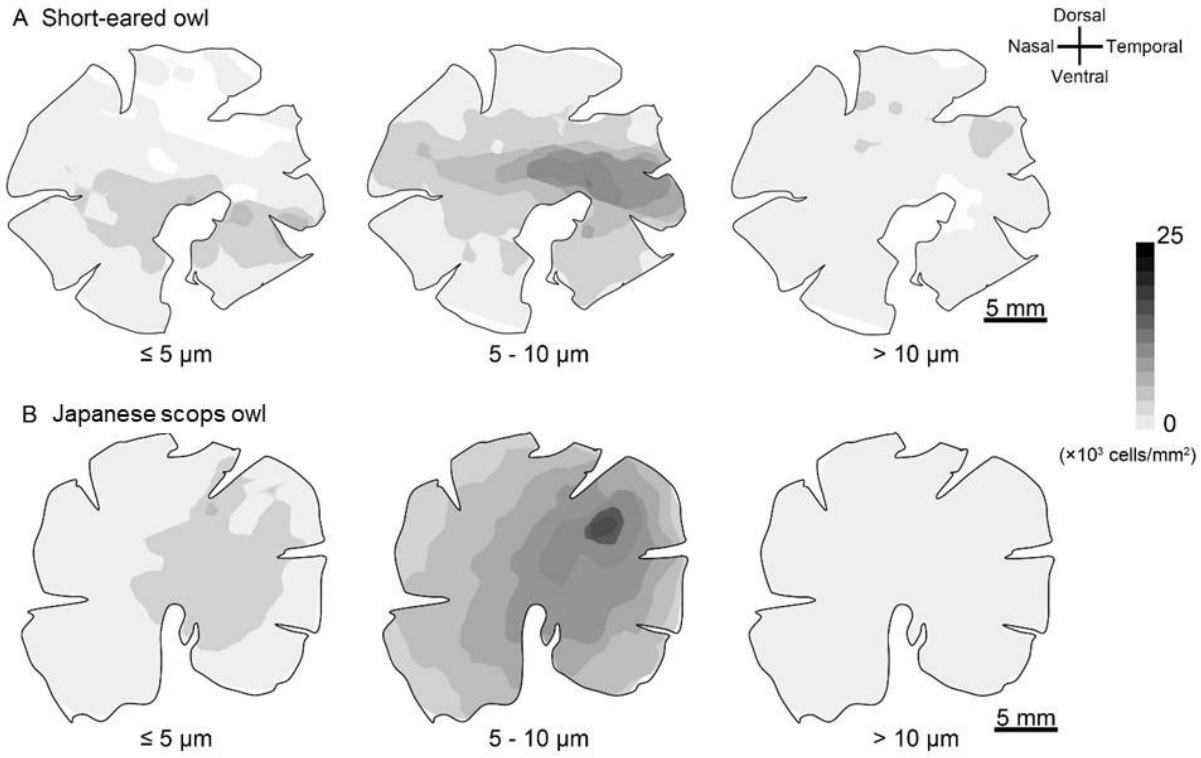

Fig. 9. The distribution of each cell group in the short-eared owl (A) and the Japanese scops owl (B).

The shaded color reveals the density scales of RGCs. Left eye. RGCs of both species were divided into three groups, that is the small- (≦5 ㎛), the medium- (5-10 ㎛), and the large-sized cells (>10 ㎛). In the short-eared owl, small-sized cells localized in the ventral area with a peak density of 6.8×10^3 cells/mm^2, and large-sized cells localized in the dorsal area with a peak density of 5.8×10^3 cells/mm^2. In the Japanese scops owl, small-sized cells localized in the dorsal area with a peak density of 6.4×10^3 cells/mm^2, while large-sized cells were uniformly distributed in the whole retina at a low density ($0.1\text{-}2.6\times10^3$ cells/mm^2). The distribution of medium-sized cells in both species was consistent with the high neural density area in the whole retina with peak densities of 17.4×10^3 and 20.2×10^3 cells/mm^2 in the short-eared owl and Japanese scops owl, respectively.

Chapter 2

Topography and morphology of retinal ganglion cells in northern goshawk (*Accipiter gentilis*).

Introduction

The northern goshawk (*Accipiter gentilis*) is a diurnal raptor ranging over Northern America, the Eurasian Continent, and Japan. The species are resident or migratory which relates to food availability in breeding areas during winter. They prefer mature forests consisting of a combination of lofty trees having intermediate canopy coverage suitable for nesting, and small, open areas within the forest for foraging. A northern goshawk prey on birds and mammals of small to moderate size, and hunt in diverse habitats ranging from open-sage steppes to forests, including riparian areas. Additionally, they are territorial species and are often extremely aggressive when defending nests from intruders (Johnsgard, 1990; Squire and Reynolds, 1997). Thus, they need highly visual performance for ecological behavior. Therefore, it is expected that the retinal topography of the northern goshawk would show the adaptation to this variety of ecological habits. So far, the RGC topography maps of diurnal predatory birds exist only for three species, American kestrel (*Falco sparverius*), black-chested buzzard-eagle (*Geranoaetus melanoleucus*), and chimango caracara *(Phalcoboenus chimango*); and little is known about that of the northern goshawk.

In Chapter 2, I conducted a histological analysis of RGCs in the northern goshawk using whole-mount preparations to obtain the retinal specialization and topography of the globose-type eye. Those results would show the adaptive feature of the eye to the ecological habit of the northern goshawk.

Materials and Methods

All experimental procedures were practiced in accordance with the Guide for the Care and Use of Experimental Animals of Iwate University (A201847, A202127).

The retina of the northern goshawk (*Accipiter gentilis*; body weight of 480.0 g) was used in this study. The injured individual had been housed in the Akita Prefectural Bird and Beast Conservation Center for a few days. The plumage was brownish overall with a streaky belly and the eyebrow was white. We found that the plumage of the individual was that of a juvenile northern goshawk (Johnsgard, 1990; Squires and Reynolds, 1997). Additionally, the body weight of the individual in this study (480 g) was smaller than those of adults, e.g., more than 631 g and 674 g for males and females, respectively (Johnsgard, 1990; Squires and Reynolds, 1997). Although the exact age is unknown, I consider the individual as a juvenile. After the unknown cause of death of the individual, I immediately removed the eye and measured the weight, corneal diameter (C) and, axial length (A) of the eye.

The preparation of the retinal whole-mount and the observation of the retina were performed as the same manner in the chapter 1.

Results

The eyes of the northern goshawk were laterally oriented on both sides of the head (Fig.10). The cornea and posterior segments of the eye were connected by scleral ossicles which characterize the globose type of eye shape (Fig. 1). The corneal diameter (C), the axial length (A), and the C:A of the northern goshawk is 13.75 mm, 20.60 mm, and 0.667, respectively. The following description was for the left eye, and I referred to the right eye in case of need for comparison. An estimate of the total number of RGCs was $4{,}427.2\times10^{3}$ in an estimated retinal area of 772 mm^2, and the distribution density of RGCs ranged between 0.7×10^3 and 22.8×10^3 cells/mm^2 (average: 5.7×10^3 cells/mm^2). Isodensity contour plots of RGCs are presented in Fig. 11. In the center of the ventral retina, the pecten which assumed the form of a feather was observed. The well-defined visual streak and two foveae, i.e., central and nasal fovea, were observed in both eyes (Fig. 11). The visual streak in the left eye was observed in the range of 10.3-22.8×10^3 cells/mm^2 and extended from a point midway between the nasal edge of the retina and the superior pole of the pecten to a point about midway between the superior pole of the pecten and the temporal edge. The visual streak included two foveal areas in the central and temporal position with the density of 22.8×10^3 and 22.7×10^3 cells/mm^2, respectively, and the superior pole of the pecten was located in between them. Around the central fovea, the radially striated arrangement of RGCs toward the center of the pit was observed, and the accumulation of RGCs in several layers was also observed at the rim of the foveal pit (Fig. 12A). On the other hand, those arrangement and accumulation of RGCs in the temporal foveal area were moderate (Fig. 12B). Most of the population of RGCs consisted of round but slightly irregular-shaped small cells around 5 μm in diameter (Fig.13A), which widely distributed over whole retina. The small cells dominated 99.6% of the total population of RGCs in the species. On the other hand, the accumulation of the large polygonal-shaped cells (> 10 μm in diameter) (Fig.13B) was brought to attention in the dorsal-, nasal-, and

temporal parts in the dorsal half of the retina (Fig. 14A). The formation of a small subset of those cells was also observed in the dorsal periphery of the left retina (Fig.14B), which was not observed in the right eye.

Discussion

The morphological features of the globose-type eye were detected in the northern goshawk. It should be mentioned that the eye morphology and retinal topography of the species here may be only applicable to the studied individual.

The organization of the retinal specialization, that is the horizontal visual streak including two foveae observed in the northern goshawk is quite the same as those of other diurnal predatory species (Inzunza et al.,1991). It is suggested that falcons and hawks may use their central foveal area for long-distance vision, i.e., monocularly side vision, and also use their temporal foveal area for short-distance vision, i.e., binocularly frontal vision (Jones et al., 2007). As the eyes of the northern goshawk orientate laterally in the head, the central and the temporal retinal area view the lateral and the frontal field, respectively. Therefore, it is assumed that the central foveal area could serve for detecting objects, such as prey and intruders in the distance; and the temporal foveal area could serve for capturing prey and attacking predators in a short distance in the binocular field.

It is reported that the neural density of the central foveal area is remarkably higher than that of the temporal foveal area in other diurnal predatory species (Inzunza et al., 1991). The retina of the American kestrel presented values for both central and temporal foveae, 65×10^3 vs. 45×10^3 cells/mm^2, respectively. Similarly, the values of 62×10^3 vs. 45×10^3 cells/mm^2 in the black-chested buzzard-eagle, and the values of 38×10^3 vs. 23×10^3 cells/mm^2 in the chimango caracara. In the present study, however, the difference between the two foveal areas in the northern goshawk is not so conspicuous (22.8×10^3 vs. 22.7×10^3 cells/mm^2), which might be caused by species, individual, age, or sex; otherwise, the counts in the region might be underestimated. Because of the densely packed accumulation and the distortion of cells, it is difficult to count cells in the central foveal area (Inzunza et al., 1991). For this reason, I counted the cells in the high-density area adjacent to the fovea, where the distortion of cells was less

observed. It is assumed that the large accumulation of cells at the rim of the central foveal pit might suggest the high resolving power in the area. The temporal fovea is located in the area around 1 mm away temporal from the temporal peak density region. Along with the hypothesis for the function of the fovea, one of an explanation for these organization in the temporal foveal area is that the temporal fovea could serve for improvement of detection and fixation on moving small objects which are to be observed by the peak density region.

Morphological classification of RGCs in birds has been demonstrated in the chick (Ueshima and Uehara, 1983; Chen and Naito, 1999) and the Japanese quail (Ikushima et al., 1986). The soma size, the population, and the topography of each cell class differ from each other in those studies, however, there showed in common that small ganglion cells dominated the first population, and the large cells were the last. In the chick, the cells with small soma represented 51.8% of the ganglion cell population, while the population of the largest cells was 2.1% (Chen and Naito, 1999). This was the same value as Ueshima and Uehara (1983) showed that the large ganglion cells dominated 2.1-2.3% of the RGCs. In the Japanese quail, the histogram of soma areas in the whole retina showed a unimodal skewed distribution, which gave 20-30 μm^2 for a peak range and more than 120 μm^2 for the lowest value (Ikushima et al., 1986). In the present study, the small cells dominated 99.6% of the population of RGCs, and the large polygonal-shaped cells dominated 0.4% of the northern goshawk.

Correspondences of the small to medium-sized cell groups of birds to the β (X) and the γ (W) cells of the cat are suggested in the chick (Ueshima and Uehara,1983) and the Japanese quail (Ikushima et al., 1986). Stone (1983) suggested that the β (X) and the γ (W) cells subserve high-resolution patterns and ambient vision, respectively. In the present study, the large population and the wide distribution of the small cells would suggest that these cells engage in viewing the whole field, i.e., ambient vision. On the other hand, it could be assumed that the concentrated population of the small cells in the visual streak would serve for high visual acuity,

i.e., high-resolution pattern vision. Therefore, the small cells in the present study might be classified into two or more groups that subserve different functional roles to each other.

It is suggested that the large RGCs in the chick (Ueshima and Uehara,1983) and the Japanese quail (Ikushima et al., 1986) correspond to the α (Y)- cells in the cat, which subserve the movement detection (Stone,1983). Foraging individuals of northern goshawk travel through the forest in a series of short flights, punctuated with brief periods of prey searching from elevated hunting perches, i.e., short duration sit-and-wait predatory movements (Squires and Reynolds, 1997). Prey in the lower fields would be viewed by the dorsal half of the retina where the accumulation of the large polygonal-shaped cells is observed. Therefore, it could be assumed that the large polygonal-shaped cells in the dorsal retina could contribute to detecting prey in the lower visual fields.

The result of Chapter 2 suggests that the horizontal visual streak and foveae observed in the northern goshawk are adapted to the inhabitation and predatory behavior of the species. The conspicuous localization of the large polygonal shaped cells observed in the northern goshawk suggests that those cells might serve for the discrimination of objects in the lower field.

Fig.10. Lateral view of the head of the northern goshawk (*Accipiter gentilis*).

The eye is laterally oriented on the head. (Right side)

The plumage of the head, the palpebra, and the skin were plucked and removed for observation.

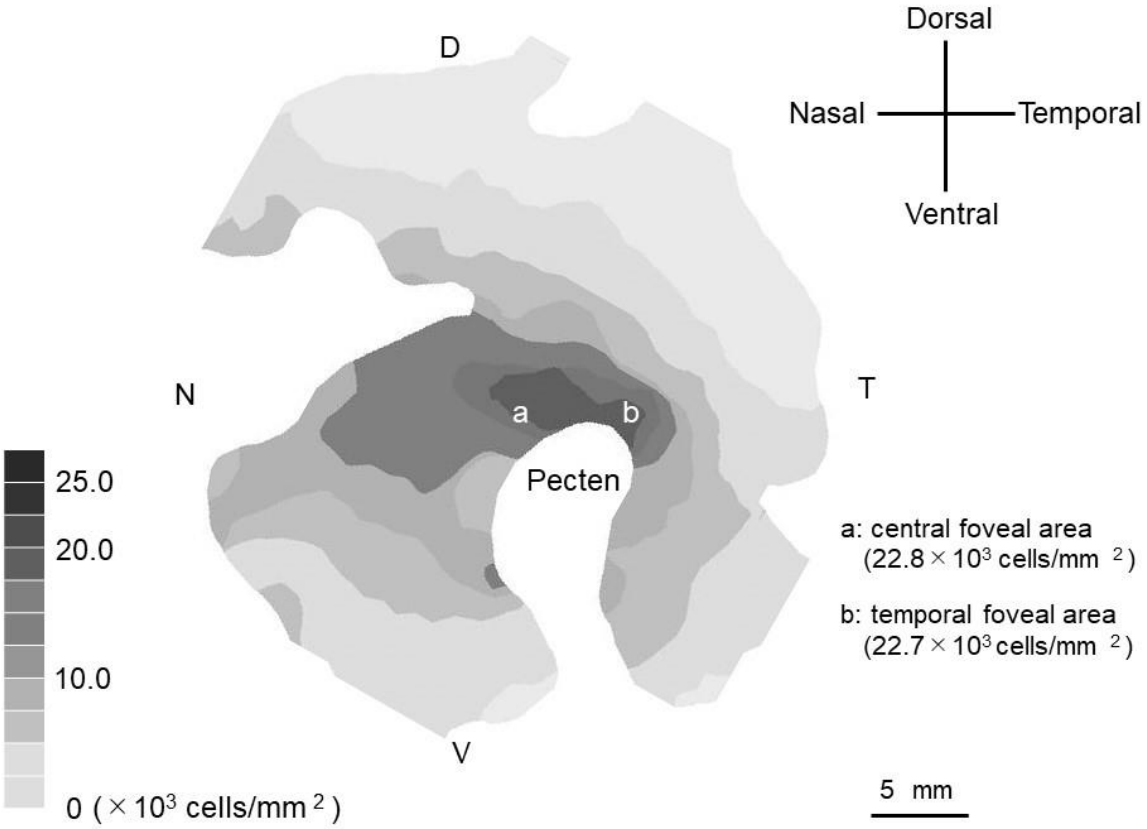

Fig. 11. Isodensity contour map of RGCs for the northern goshawk.

The shaded color reveals the density scales of RGCs. Bars represent 5 mm. Left eye.

The distribution density of RGCs ranged between 0.7×10^3 and 22.8×10^3 cells/mm^2 (average: 5.7×10^3 cells/mm^2). The distribution of RGCs skew to the temporal area, where the binocularly visual field would be projected. The density of RGCs steeply decreases toward the dorsoventral direction in the retina.

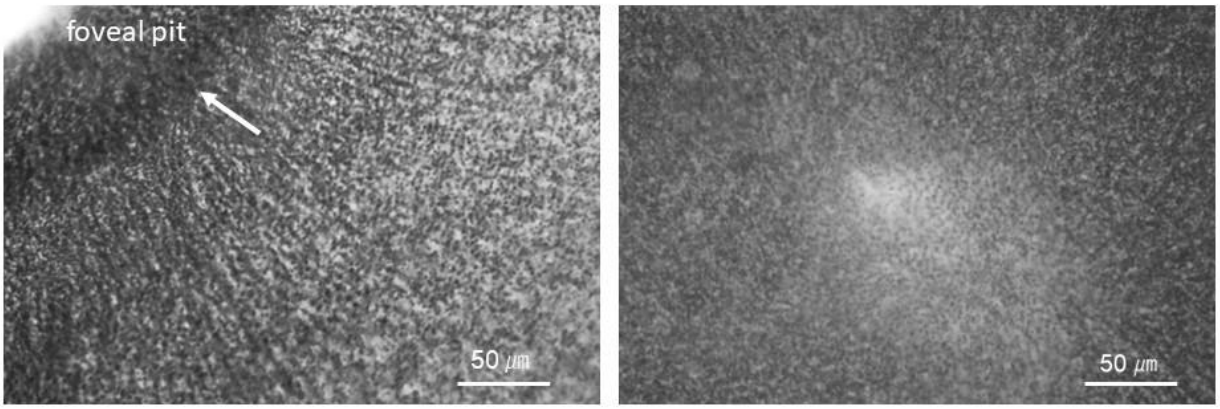

A: Central fovea B: Temporal fovea

Fig. 12. Microphotographs of the central fovea (A) and the temporal fovea (B) in the northern goshawk.

The central foveal pit is located in the upper left of the left photograph (A). Radially striated arrangement of the RGCs is observed in the central foveal area. The large accumulation and the distortion of the cells are observed in the foveal rim (white arrow), on the other hand, that organization is moderate in the temporal foveal region (B). Bars represent 50 μm.

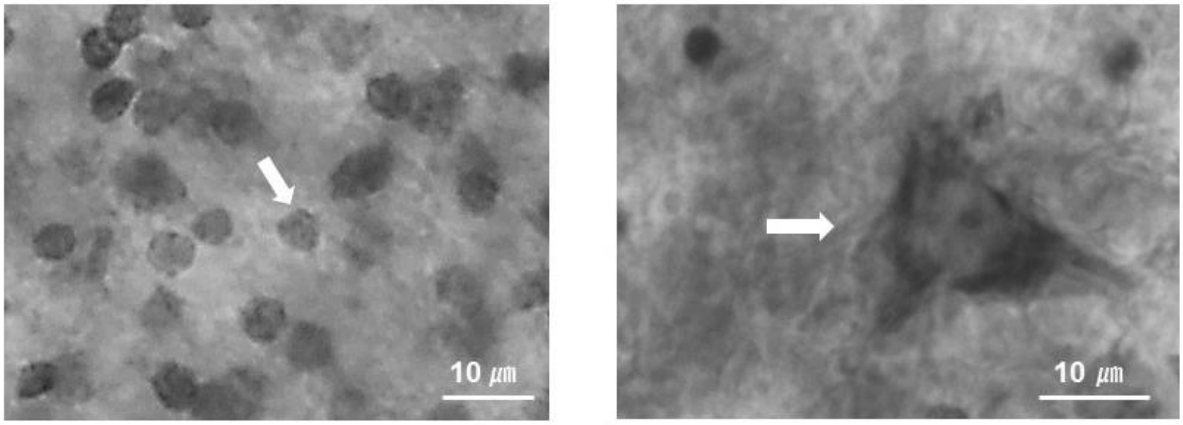

A: Temporal area B: Dorsal area

Fig. 13. Microphotograph of the RGCs in the temporal area (A) and the dorsal area (B) in the northern goshawk.

Most of the population of RGCs consisted of round but slightly irregular-shaped small cells (arrow, A), which are widely distributed over the whole retina. The small cells dominated 99.6% of the population of RGCs. The large polygonal-shaped large cells with cytoplasmic Nissl substance and large nuclei (arrow, B). The population of the large cells is 0.4% of the population of RGCs.

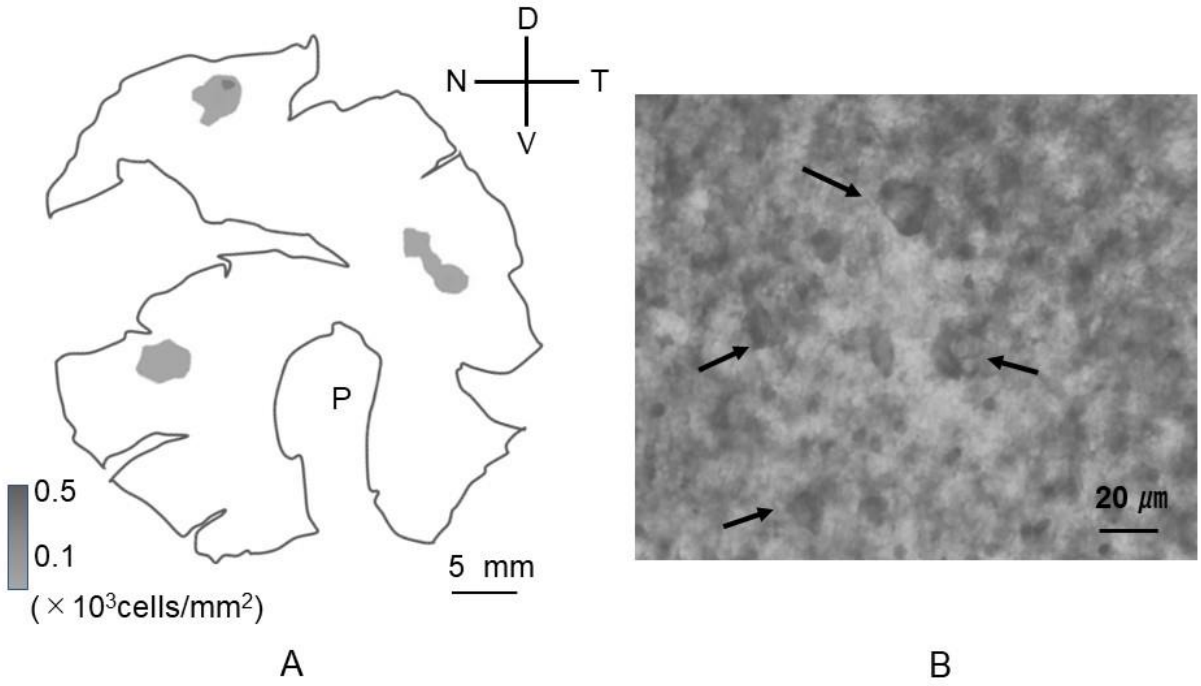

Fig. 14. Isodensity contour maps of the large cells (A), and microphotograph of a small subset of the large cells in the dorsal retina (B) in the northern goshawk.

The localization of the large RGCs is observed in the dorsal, nasal, and temporal periphery of the retina (A). A small subset composed of eight to ten large cells (arrows) is observed in the dorsal periphery of the left retina (B: 0.5 $\times 10^3$ cells/mm^2).

D, Dorsal; V, Ventral; N, Nasal; T, Temporal direction; P, Pecten.

General discussion

The present results may indicate that the morphological diversity of the eyes in three species of predatory bird is adaptable to the ecological behavior and feeding habits. It is speculated that adaptation of eye morphology and the RGC topography have appeared even in the tubular- and globose-type eyes. The results of the present study are summarized in Table 2.

The C:A for the northern goshawk is smaller than that of the two species of owl. On the other hand, the C:A of the short-eared owl is larger or similar to that of the Japanese scops owl. This result would show that the C:A indicates the difference between the species with the globose type and the tubular type of eye. However, it would not indicate the apparent difference between the crepuscular and the nocturnal species with the tubular type of eye.

The retinal area of the northern goshawk is larger than those of the two species of owl. On the other hand, the axial length of the eye in the Japanese scops owl and the northern goshawk is similar to each other. The result would show that the retinal area of the eye of globose type is larger than its eye size compared to that of the tubular type of eye. A large retinal area enables the species to observe a lot of objects in the wide field. Therefore, the large retinal area in the northern goshawk would be available for the predatory behavior of the species. As shown in Fig.3., the size of the posterior segments of the owl's eyes are constrained in the skull. Therefore, the size of the retina in the posterior segments of the eye is also limited, then, the population of RGCs would be densely packed on the retina in the eye of tubular type. Consequently, the density of RGCs in the peripheral retina of two owls is not so lower as that of the northern goshawk. The result indicates that the two owls could exhibit their resolving power over the whole visual field. The binocularly overlapped vision in the frontal-oriented eye of the owl would be enhanced by the high resolving power of both eyes. Those organizations could accommodate the species to detect and capture prey in a short distance under dim light conditions; that is the predatory behavior of the owls.

In the northern goshawk, the density of RGCs steeply decreases toward the peripheral retina, especially in the dorso-ventral direction, compared to that of the owls. The result suggests that the northern goshawk would obviously lose resolving power in the periphery of the visual field. The northern goshawk could rapidly approach the objects by its high flight performance, then, the image of an object in a short distance would easily be projected onto the visual streak. Therefore, it is assumed that the high flight performance of the northern goshawk could supplement the low resolving power in the periphery of the visual field.

Among the RGCs in the three species in the present study, the large RGCs are distinct from other RGCs in the shape and soma size. In the short-eared owl and the northern goshawk, the localization of the large RGCs is observed in the dorsal retina. Those retinal areas would view the lower field in which prey are detected for both species. On the other hand, in the Japanese scops owl, the large RGCs are distributed over the whole retina with low density. The visual field for the Japanese scops owl is obscured by trees, then, the species could search for prey in the whole visual field. It has been suggested that the large RGCs might relate to the movement detection in birds (Ueshima and Uehara,1983; Ikushima et al., 1986). Therefore, it could be assumed that the large RGCs in the three species might be involved in detecting prey. As a result, the topography of the large RGCs would be adaptable to the foraging behavior of each species.

In conclusion, the retinal specialization which is observed in the globose and tubular type of eyes is adaptable for the inhabitation and the feeding habit of each species. The density of RGCs in the retinal periphery of each species shows the specific feature, which is lower in the globose type and higher in the tubular type of eye.

Table 2. Summary of retinal topography data in the short-eared owl, the Japanese scops owl, and the northern goshawk

Species	Retinal area (mm^2)	Total number of RGCs ($\times 10^3$ cells)	Peak cell density ($\times 10^3$ cells/mm^2)	Average cell density ($\times 10^3$ cells/mm^2)	RGCs' density in the peripheral area ($\times 10^3$cells/mm^2)			
					Dorsal	Ventral	Temporal	Nasal
Short-eared owl	336	2,342.0	17.4	7.0	4.0 - 6.0	4.0 - 6.0	12.0 -14.0	6.0 - 8.0
Japanese scops owl	428	4,703.0	23.1	11.0	10.0 - 12.0	10.0 - 12.0	10.0 - 12.0	8.0 - 10.0
Northern goshawk	772	4,427.2	22.8	5.7	< 2.5	< 2.5	2.5 - 5.0	5.0 - 7.5

Acknowledgements

I am profoundly grateful to the chief supervisor Dr. Yoshio Yamamoto, Professor, Laboratory of Veterinary Anatomy, Iwate University for his scholastic guidance, sympathetic encouragement, and valuable advice.

I express cordial respect and sincere thanks to the co-supervisor, Associate Professor Masahiro Kaneda, Tokyo University of Agriculture and Technology and Associate Professor Nobuaki Nakamuta, Iwate University.

My sincere gratitude is due to Dr. Hideshi Shibata, the former professor at Tokyo University of Agriculture and Technology for helpful management and support to accomplish this study.

Grateful acknowledgement is made to Professor Kentaro Nagaoka, Tokyo University of Agriculture and Technology and Professor Keiichiro Kizaki, Iwate University for constructive suggestions and criticism to this thesis.

I feel much pleasure to convey my thanks to Chief Officer Tomoko Akagawa at the Nature Maintenance Division of Akita Prefectural Office, and the entire member of the Akita Prefectural Bird and Beast Conservation Center.

References

Bird Life International. (2019) https//www.birdlife.org/birds/owls/ (accessed 27 November 27, 2020)

Bishop GH and O'Leary JS. (1938). Potential records from the optic cortex of the cat. J Neurophysiol. **1**: 391-404.

Bishop GH and O'Leary JS. (1940). Electrical activity of the lateral geniculate of cats following optic nerve stimuli. J Neurophysiol. **3**: 308-322.

Bishop GH and O'Leary JS. (1942). Factors determining the form of the potential record in the vicinity of the synapse of the dorsal nucleus of the lateral geniculate body. J Cell Comp Physiol. **3**: 315-331.

Boycott BB and Wässle H. (1974). The morphological types of ganglion cells of the domestic cat's retina. J Physiol. **240**: 397-419.

Bravo H and Pettigrew JD. (1981). The distribution of neurons projecting from the retina and visual cortex to the thalamus and tectum opticum of the barn Owl, *Tyto alba,* and the burrowing owl, *Speotyto cunicularia*. J Comp Neurol. **199**: 419-441.

Brooke M.de L, Hanley S and Laughlin SB. (1999). The scaling of eye size with body mass in birds. Proc R Soc B Biol Sci. **266**: 405-412.

Burton RF. (2008). The scaling of eye size in adult birds: Relationship to brain, head and body sizes. Vision Res. **48**: 2345-2351.

Calderone JB, Reese BE and Jacobs GH. (2003). Topography of photoreceptors and retinal ganglion cells in the spotted hyena (*Crocuta crocuta*). Brain Behav Evolv. **62**: 182-192.

Carpenter JW, Mashima TY and Rupiper DJ. Exotic Animal Formulary, 2nd ed., 2001. WB Saunders, Philadelphia.

Chen Y and Naito J. (1999). Morphological classification of ganglion cells in the central retina of chicks. J Vet Med Sci. **61**: 537-542.

Cleland BG, Dubin MW and Levick WR. (1971). Sustained and transient neurones in the cat's retina and lateral geniculate nucleus. J Physiol. **217**: 473-496.

Coimbra JP, Trévia N, Marceliano MLV, Andrade-da-costa BLdaS, Pcanço-diniz CW and Yamada ES. (2009). Number and distribution of neurons in the retinal ganglion cell layer in relation to foraging behaviors of Tyrant Flycatchers. J Comp Neurol. **514**: 66-73.

Coimbra JP, Nolan PM, Collin SP and Hart NS. (2012). Retinal ganglion cell topography and spatial resolving power in penguins. Brain Behav Evol. **80**: 254-268.

Collin SP and Pettigrew JD. (1988). Retinal topography in reef teleosts. Brain Behav Evol. **31**: 283-295.

Collin SP. Behavioural ecology and retinal cell topography. 1999; pp. 509-535. In: Adaptive Mechanisms in the Ecology of Vision. (Archer SN, Djamgoz MBA, Loew ER, Patridge JC, Vallerga S eds.) Dordrecht: Kluwer Academic Publishers.

Collin SP. (2008). A web-based archive for topographic maps of retinal cell distribution in vertebrates. Clin Exp Optom. **91**: 85-95.

Dunlop SA, Longley WA and Beazley LD. (1987). Development of the area centralis and visual streak in the grey kangaroo *Macropus fuliginosus.* Vision Res. **27**: 151-164.

Ehrlich D. (1981). Regional specialization of the chick retina as revealed by the size and density of neurons in the ganglion cell layer. J Comp Neurol. **195**: 643-657.

Enroth-Cugell C and Robson J G. (1966). The contrast sensitivity of retinal ganglion cells of the cat. J Physiol. **187**: 517-552.

Fernández-Juricic E, Moore BA, Doppler M, Freeman J, Blackwell BF, Lima SL and DeVault

TL. (2011). Testing the terrain hypothesis: Canada geese see their world laterally and obliquely. Brain Behav Evol.**77**: 147-158.

Fishelson L, Ayalon G, Zverdling A and Holzman R. (2004). Comparative morphology of the eye (with particular attention to the retina) in various species of Cardinal Fish (Apogonidae, Teleostei) Anat Rec A Discov Mol Cell Evolv Biol. **277A**: 249 -261.

Garamszegi LZ, Møller AP and Erritzøe J. (2002). Coevolving avian eye size and brain size in relation to prey capture and nocturnality. Proc R Soc Lond B Biol Sci. **269**: 961-967.

Gundersen HGJ. (1977). Notes on the estimation of the numerical density of arbitrary profiles: the edge effect. J Microsc. **111**: 219-223.

Hall MI and Ross CF. (2007). Eye shape and activity pattern in birds. J Zool. **271**: 437-444.

Hall MI. (2008). Comparative analysis of the size and shape of the lizard eye. Zool. **111**: 62-75.

Hart NS. (2002). Vision in the peafowl (Aves: *Pavo cristatus*). J Exp Biol. **205**: 3925-3935.

Hebel R. (1976). Distribution of retinal ganglion cells in five mammalian species (pig, sheep, ox, horse, dog). Anat Embryol. **150**: 45-51.

Heesy CP and Hall MI. (2010). The nocturnal bottleneck and the evolution of mammalian vision. Brain Behav Evol. **75**:195-203.

Holden AL. (1977). Responses of directional ganglion cells in the pigeon retina. J Physiol. **270**: 253-269.

Howland HC, Merola S and Basarab JR. (2004). The allometry and scaling of the size of vertebrate eyes. Vision Res. **44**: 2043-2065.

Hughes A. The topography of vision in mammals of contrasting life style: comparative optics and retinal organization. 1977; pp 613-756. In: Handbook of sensory physiology, vol VII/5 (Cresitelli F. ed) Springer, Berlin Heidelberg, New York.

Ikushima M, Watanabe M, and Ito H. (1986). Distribution and morphology of retinal ganglion cells in the Japanese Quail. Brain Res. **376**: 320-334.

Inzunza O, Bravo H, Smith RL, Angel M. (1991). Topography and morphology of retinal ganglion cells in Falconiforms: a study on predatory and carrion-eating birds. Anat Rec. **229**: 271-277.

IUCN (2021). The IUCN Red List of Threatened Species. Version 2021-1. (accessed May 31, 2021).

Johnsgard PA. (1988). North American Owls: Biology and Natural History. Paul Johnsgard Collection. Smithsonian Institution Press, Washington and London.

Johnsgard, P.A. (1990). Hawks, eagles & falcons of North American Biology and natural history. Retrieved from http://digitalcommons.unl.edu/johnsgard (accessed 1 November 2019).

Jones MP, Pierce Jr KE and Ward D. (2007). Avian vision: a review of form and function with special consideration to birds of prey. J Exot Pet Med.**16**: 69-87.

Kiltie RA. (2000). Scaling of visual acuity with body size in mammals and birds. Funct Ecol. **14**: 226-234.

Kirk EC. (2004). Comparative morphology of the eye in primates. Anat Rec Discov Mol Cell Evolv Biol. **281A**: 1095-1103.

Kirk EC. (2006a). Effects of activity pattern on eye size and orbital aperture size in primates. J Hum Evol. **51:** 159-170.

Kirk EC. (2006b). Eye morphology in cathemeral lemurids and other Mammals. Folia Primatol. **77**: 27-49.

Kolb H, Nelson R, Ahnelt P and Cuenca N. (2001). Cellular organization of the vertebrate retina. Prog Brain Res. **131**: 3-26.

Kuffler SW. (1953). Discharge patterns and functional organization of mammalian retina. J Neurophysiol. **16**:37-38.

Land MF and Fernald RD (1992). The evolution of eyes. Annu. Rev. Neurosci. **15**: 1-29.

Lisney TJ, Iwaniuk AN, Bandet MV and Wylie DR. (2012). Eye shape and retinal topography in owls (Aves: Strigiformes). Brain Behav Evol. **79**: 218-236.

Lisney TJ, Stecyk K, Kolominsky J, Graves GR, Wylie DR, and Iwaniuk AN. (2013a). Comparison of eye morphology and retinal topography in two species of new world vultures (Aves:Cathartidae). Anat Rec. **296**: 1954-1970.

Lisney TJ, Stecyk K, Kolominsky J, Schmidt BK, Corfield JR, Iwaniuk AN and Wylie DR. (2013b). Ecomorphology of eye shape and retinal topography in waterfowl (Aves: Anseriformes: Anatidae) with different foraging modes. J Comp Physiol A. **199**: 385-402.

Lisney TJ, Wylie DR, Kolominsky J and Iwaniuk AN. (2015). Eye morphology and retinal topography in Hummingbirds (Trochilidae: Aves). Brain Behav Evol. **86**: 176-190.

Malmström T and Kröger RHH. (2006). Pupil shapes and lens optics in the eyes of terrestrial vertebrates. J Exp Biol. **209**: 18-25.

Martin GR. (1982). An Owl's Eye: Schematic Optics and Visual Performance in *Strix aluco L.* J Comp Physiol. **145**: 341-349.

Martin GR. (1983). Schematic eye models in vertebrates. In Progress in sensory physiology vol 4. pp 43-81.

Martin GR. (1986). Sensory capacities and the nocturnal habit of owls (Strigiformes). Ibis. **128**: 266-277.

Martin GR. (1994). Form and structure in the optical structure of bird eyes. 1994; pp 5-34. In Perception and motor control in birds. 1st ed. (Davies MNO and Green PR eds.), Springer, Berlin, Heidelberg.

Martin GR and Osorio D. Vision in birds. 2008; pp 25-52. In: The senses. Vol1. (Masland RH and Albright TD eds.) Academic Press, London.

Mass AM and Supin AY. (2007). Adaptive features of aquatic mammal's eye. Anat Rec. **290**:

701-715.

Meyer DB. (1977). The avian eye and its adaptations. 1977; pp. 549-612. In: The visual system of vertebrates. Handbook of sensory physiology Vol.VII/5. (Crescitelli F. ed.). New York: Springer-Verlag.

Mitkus M, Poiter S, Martin GR, Duriez O and Kelber A. (2018). Raptor vision. Oxford research encyclopedia of neuroscience.

Website: https://doi.org/10.1093/acrefore/9780190264086.013.232 (accessed December 20, 2019).

Motani R and Schmitz L. (2011). Phylogenetic versus functional signals in the evolution of form-function relationships in terrestrial vision. Evolution. **65**: 2245-2257.

Murphy CJ and Howland HC. (1987). The optics of comparative ophthalmoscopy. Vision Res **27**: 599-607.

Peterson EH and Ulinski PS. (1979). Quantitative studies of retinal ganglion cells in a turtle, *Pseudemys scripta elegans*. I. number and distribution of ganglion cells. J Comp Neurol. **186**: 17-42.

Poiter S, Mitkus M and Kelber A. (2020). Visual adaptations of diurnal and nocturnal raptors. Semin Cell Dev Biol. **106**: 116-126.

Pumphrey RJ. (1948). The theory of the fovea. J Exp Biol. **25**: 299-312.

Pumphrey RJ. (1961). Sensory Organs: Vision. pp. 55-68. In: Biology and Comparative Physiology of BIRDS. Vol. II. 2nd ed. (Marshall AJ.ed.) Academic Press, New York & London.

Rahman ML, Sugita, S, Aoyama M, Sugita S. (2006). Number, distribution and size of retinal ganglion cells in the jungle crow (*Corvus macrorhynchos*). Anat Sci Int. **81**: 253-259.

Rahman ML, Kuroda K, Aoyama M and Sugita S. (2010). Regional specialization of the ganglion cell density in the retina of the ostrich (*Struthio camelus*). Anim Sci J. **81**: 108-115.

Ross CF, Hall MI and Heesy CP. (2007). Were basal primates nocturnal? Evidence from eye and orbit shape. 2007; pp. 233-256. In: Primate origins: Adaptations and evolution. 1st ed. (Ravosa MJ and Dagosto M. eds.), Springer, Boston, MA.

Ross CF and Kirk EC. (2007). Evolution of eye size and shape in primates. J Hum Evol. **52**: 294-313.

Rowe M H and Stone J. (1976). Properties of ganglion cells in the visual streak of the cat's retina. J Comp Neurol. **167**: 99-126.

Schmitz L. (2009). Quantitative estimates of visual performance features in fossil birds. J Morphol. **270**: 759-773.

Schmitz L and Motani R. (2010). Morphological differences between the eye balls of nocturnal and diurnal amniotes revisited from optical perspectives of visual environments. Vision Res. **50**: 936-946.

Shapley R and Perry VH. (1986). Cat and monkey retinal ganglion cells and their visual functional roles. Trends Neurosci. **9**: 229-235.

Squires JR and Reynolds RT. Northern Goshawk. 1997; pp. 1-31. In: The Birds of North America. 298. Washington DC: The Academy of Natural Sciences Philadelphia, PA; The American Ornithologists' Union.

Stone J and Hoffman K-P. (1972). Very slow-conducting ganglion cells in the cat's retina: a major, new, functional type? Brain Res. **47**: 610-616.

Stone J and Fukuda Y. (1974). Properties of cat retinal ganglion cells: a comparison of W-cells with X-and Y-cells. J Neurophysiol. **37**: 722-748.

Stone J. (1983). Parallel Processing in the Visual System (Perspectives in Vision Research).1 st

ed. (Blakemore C. ed.). Plenum Press, New York.

Thomas RJ, Széskely T, Cuthill IC, Harper DGC, Newson SE, Frayling TD and Wallis PD. (2002). Eye size in birds and the timing of song at dawn. Proc R Soc Lond B. **269**: 831-837.

Thomas RJ, Kelly DJ and Goodship NM. (2004). Eye design and visual constraints on behavior. Ornitol Neotrop. **15**: 243-250.

Thomas RJ, Széskely T, Powell RF and Cuthill IC. (2006). Eye size, foraging methods and the timing of foraging in shorebirds. Funct Ecol. **20**: 157-165.

Ueshima T and Uehara M. (1983). Distribution of the α-type ganglion cells in the chicken retina. Jpn J Vet Sci. **45**: 289-295.

Ullman JFP, Moore BA, Temple SE, Juricic EF and Collin SP. (2012). The retinal wholemount technique: a window to understanding the brain and behaviour. Brain Behav Evol. **79**: 26-44.

Veilleux CC and Kirk EC. (2014). Visual acuity in mammals: Effects of eye size and ecology. Brain Behav Evol. **83**: 43-53.

Walls GL. (1942). The Vertebrate eye and Its Adaptive Radiation. Bloomfield Hills, Cranbrook Institute of Science. (accessed December 20, 2020).

Wathey JC and Pettigrew JD. (1989). Quantitative analysis of the retinal ganglion cell layer and optic nerve of the barn owl *Tyto alba*. Brain Behav Evol. **33**: 279-292.

Wilhelm M and Straznicky C. (1992). The topographic organization of the retinal ganglion cell layer of the lizard *Ctenophorus nuchalis*. Arch Histol Cytol. **55**: 251-259.